Pergamon

J. Mech. Phys. Solids, Vol. 44, No. 12, pp. 2079–2102, 1996

0022–5096/96 $15.00+0.00

PII: S0022–5096(96)00058–0

THE FRACTAL CRUSHING OF GRANULAR MATERIALS

G. R. MCDOWELL, M. D. BOLTON and D. ROBERTSON

Department of Engineering, University of Cambridge, U.K.

(*Received* 27 *June* 1995; *in revised form* 5 *April* 1996)

ABSTRACT

A study has been made of the micro mechanical origins of the irrecoverable compression of aggregates which comprise brittle grains. The terms "yielding" and "plastic hardening" are used in the discipline of soil mechanics to describe the post-elastic behaviour of granular media. These "plastic" phenomena are here related to the successive splitting of grains.

Grains are taken to split probabilistically, the likelihood increasing with applied (macroscopic) stress, but reducing with any increase in the co-ordination number and with any reduction in particle size. When the effect of the co-ordination number dominates, a simple numerical model confirms published findings that a fractal distribution of particle sizes evolves from the compression of an aggregate of uniform grains.

Taking the production of new surface area from the particle size distributions produced by the numerical model, a work equation is used to deduce the plastic compression of voids, for one-dimensional compression of the aggregate. This too is shown to be in agreement with experimental data, and in particular confirms the linearity of plots of voids ratio versus the logarithm of stress. The gradient of these plots is for the first time related to fundamental material parameters.

Keywords: A. fracture, A. fractals, B. constitutive behaviour, B. granular material, C. probability and statistics.

1. INTRODUCTION

From the earliest publications in soil mechanics, it has been accepted that the one-dimensional plastic compression of granular media satisfies an approximately linear relationship between voids ratio e (volume of voids per unit volume of solids) and the logarithm of effective macroscopic compressive stress $\bar{\sigma}$:

$$e = e_0 - \lambda \ln \bar{\sigma}. \tag{1}$$

This linearity applies to a wide range of granular materials (Novello and Johnston, 1989). However (1) is dimensionally problematical—one might have expected that the stress $\bar{\sigma}$ should be made non-dimensional by dividing it by a material parameter with dimensions of stress. Furthermore, the micro mechanical origins of the compression index λ remain to be clarified. There is now strong evidence (Lee and Farhoomand, 1967; Billam, 1971; Miura and O-Hara, 1979; Biarez and Hicher, 1994) to show that large strain deformations of granular media are accompanied by grain crushing. Suppose, therefore, that grain crushing lies behind the phenomenon of the plastic compression of brittle, granular media.

The crushing of particles in a granular material must be related to changes in the

particle size distribution (Hardin, 1985). There are two approaches for predicting particle size distributions: constrained and unconstrained comminution models. Unconstrained models assume that each particle acts independently of its neighbours. Gilvarry (1961, 1964) showed that if particles contain a Poisson distribution of flaw sizes, the distribution of fragment sizes following a succession of independent fractures is given by:

$$\Phi_{L<d} = 1 - e^{-d/x}, \tag{2}$$

where $\Phi_{L<d}$ is the cumulative fraction of the initial volume corresponding to particles of size less than d, and x is a measure of mean edge flaw spacing. Epstein (1949) developed an unconstrained model by assuming each particle to have the same probability of breakage, independent of its size or history, and that the distribution of pieces resulting from repeated fracture of a single particle was independent of its size. He showed, using the Central Limit Theorem, that any initial particle distribution, no matter how skewed, will eventually tend to a log-normal distribution.

Turcotte (1986) found that for many granular materials, the particle size distributions are self-similar and not log-normal. Sammis *et al.* (1987) found this to be true for gouge material, and stated that the weaker larger particles had not disappeared. Consequently they developed a constrained comminution model, based on the idea that a particle's fracture probability is not controlled by its intrinsic strength, but by the relative sizes of its nearest neighbours. They proposed that the load distribution for all particles would be maximised by a self-similar distribution of particles, arranged such that nearest particles were of different sizes. Once self-similarity is achieved, particles at all orders would have the same probability of failure and hence self-similarity would be maintained.

Palmer's model for the fractal crushing of ice (Palmer and Sanderson, 1991) assumed a probability of fracture which is constant at all orders, and related the crushing force on a block of ice to the fracture probability, the number of fragments into which a particle splits (assumed constant at all orders) and the number of orders. Palmer and Sanderson assumed the fracture probability for a particle to be independent of its size and number of neighbours, and stated that such a criterion would lead to a self-similar arrangement in which nearest neighbours are of different sizes.

It is well known that the crushing strength of a particle *is* a function of its size (Billam, 1972; Lee, 1992). Furthermore, if a particle has a high co-ordination number (number of contacts with neighbours), the load on it is well distributed and the probability of fracture is much lower than that at low co-ordination numbers. In addition, particles are more likely to crush as the stress on a sample of granular material increases. As yet, it is not known of any attempt to model grain crushing based on all three of these criteria.

The study of large populations, based on simple propositions for the behaviour of individuals and the interaction between neighbours, can reveal the unexpected emergence of "rules" governing the behaviour of the population as a whole (McGlade, 1993). Here, the existence of approximately linear compression lines for granular materials when voids ratio is plotted against the logarithm of applied stress, is the emergent property of interest.

In order to establish a demonstration of the principles involved, a highly simplified two-dimensional numerical model (GRANALOGY) is introduced. The initial sample of material in the model comprises uniformly sized grains. The grains are allowed to split, probabilistically, depending on the applied stress and the co-ordination number and size of each particle. These grains are seen as triangular laminae in the model, but are intended to represent real soil particles, in rather the same way that Palmer and Sanderson (1991) used a hierarchy of splitting cubes to model the crushing of ice. The particle size distribution is seen to evolve with increasing applied macroscopic stress, and the resulting distributions are analysed and discussed. Information regarding the evolution of particle distributions is expressed in terms of their co-ordination number, size, surface area and volume. This is then translated back into terms which are meaningful with respect to a real aggregate of grains with voids. The energy absorbed in the creation of new surface is taken from the model and inserted into a 3D work equation which also includes the frictional dissipation due to the rearrangement of particles. This is solved for one-dimensional compression to calculate the reduction in voids ratio with increasing applied stress. The resulting curves are compared to experimental data and, finally the compressibility of the aggregate is related to the more fundamental properties of the particles themselves.

2. THEORY

The initial sample of granular material appears as an array of 50 identical isosceles right-angled triangles (Fig. 1). Each particle (triangle) can then split into two identical self-similar triangles, and so on. This geometry has no particular significance, except to allow the fragments to be geometrically similar, but of different sizes. It should be

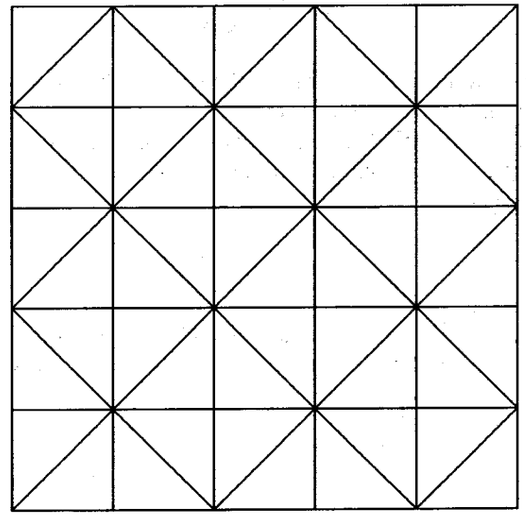

Fig. 1. Initial array of 50 identical right-angled isosceles triangles.

noted that this model does not deal with local equilibrium or kinematics, but simply with the probability of splitting of grains of known co-ordination.

The model for breakage is based on Weibull statistics of fracture (Weibull, 1951). Weibull recognises that the survival of a block of material under tension requires that all its constituent parts remain intact. Weibull stated that, for a block of material of volume V, under an applied tensile stress σ, the "survival probability" $P_s(V)$ of the block is given by:

$$P_s(V) = \exp\left\{-\frac{V}{V_0}\left(\frac{\sigma}{\sigma_0}\right)^m\right\}. \tag{3}$$

V_0 is the volume of material such that

$$P_s(V_0) = \exp\left\{-\left(\frac{\sigma}{\sigma_0}\right)^m\right\}, \tag{4}$$

where σ_0 is the value of σ such that 37% of the total number of tested blocks survive. The exponent m is called the Weibull modulus, which increases with decreasing variability in strength of the material. For chalk, brick, stone, pottery and cement, m is about 5. A similar value would be expected for carbonate sands, which have similar intraparticle porosity values. The engineering ceramics have values for m of about 10, and the variation in strength is much less.

If particles are geometrically similar, and also have the same number and distribution of contacts, the size of the zones of the tensile stress induced in them will scale with their volume. In that case Weibull applies. If particles are all initially size d_0 and we assume that there is some characteristic mobilised tensile stress σ within each of them, then the probability of survival for a particle of size d is given by:

$$P_s(d) = \exp\left\{-\left(\frac{d}{d_0}\right)^w\left(\frac{\sigma}{\sigma_0}\right)^m\right\}. \tag{5}$$

For real three-dimensional grains we must take $w = 3$, whereas in the simple arrangement of triangular laminae, "volume" is represented as plan area and $w = 2$. Equation (5) gives the variation in particle strength with particle size. When a spherical grain is loaded diametrically under a pair of forces F, the characteristic tensile stress induced within it can be defined as

$$\sigma = \frac{F}{d^2}, \tag{6}$$

following Jaeger (1967). This is also consistent with the definition of the tensile strength of concrete in the Brazilian test. Lee used this to calculate the tensile stress at fracture as

$$\sigma_f = \frac{F_f}{d^2}, \tag{7}$$

which he found to be a function of d:

$$\sigma_f \propto d^b, \tag{8}$$

where typical values of b, he found, were -0.357, -0.343, -0.420 for Leighton Buzzard sand, oolithic limestone and carboniferous limestone, respectively. Equations (5) and (8) are equivalent in the sense that if a standard probability of survival is used to define σ_f for various batches of grains of different diameter d, it will be found that

$$d^w\sigma_f^m = \text{constant}, \tag{9}$$

so that

$$\sigma_f \propto d^{-3/m}, \tag{10}$$

taking $w = 3$ for solid particles. Apparently, a value of m in the range 5–10 covers Lee's data for rock grains.

Once particles begin to split it is necessary to modify (5) to account for variable co-ordination number. The mobilised tensile stress at a characteristic point in a particle must be a function of the macroscopic stress $\bar{\sigma}$ and the co-ordination number C. Jaeger (1967) analysed circular particles under combinations of surface forces and showed that the maximum tensile stress in a particle reduces as C increases. $C = 1$ is meaningless for particles carrying contact forces, and $C = 2$ is impossible in our simple model of close-packed triangles for which C takes its minimum possible value of 3 in the initial case of an array of identical particles. A regular cubical array of spherical particles, all of diameter d, under uniaxial macroscopic stress $\bar{\sigma}$ would create a minimum possible co-ordination and would effectively load each particle diametrically with a compressive force $F = \bar{\sigma}d^2$. This would lead to the induction of a tensile stress within each particle equal to the macroscopic compressive stress on the aggregate

$$\sigma = \bar{\sigma} \tag{11}$$

following (6). In order to achieve an equivalence between the 2D analogue and this simple 3D example, it is necessary to have $\sigma = \bar{\sigma}$ for $C = 3$. We might therefore write:

$$\sigma = \frac{\bar{\sigma}}{(C-2)^\alpha}, \tag{12}$$

where the α-factor can be used to vary the degree to which the co-ordination number affects the tensile stress induced in a particle. For example, a large value of C will be more helpful in reducing the induced tensile stress for a rounded particle than for an angular particle, as indicated diagrammatically in Fig. 2. It may be possible, then, to relate α to the shape factor for a particular granular material.

Finally, the criterion for 2D fracture is given by putting (12) into (5) for $w = 2$:

$$P_s(d) = \exp\left\{-\left(\frac{d}{d_0}\right)^2\frac{(\bar{\sigma}/\sigma_0)^m}{(C-2)^a}\right\}, \tag{13}$$

where

$$a = \alpha m. \tag{14}$$

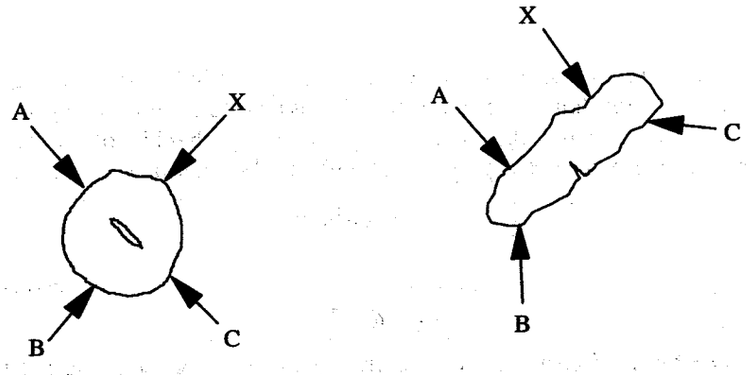

Fig. 2. Large co-ordination numbers are less helpful for more angular particles.

Figure 1 should be accepted as a logical map of the neighbourhood relationships of particles which satisfy (13) with regard to their probability of survival under macroscopic stress $\bar{\sigma}$. This statistical model permits us to calculate the work done due to the creation of surface area as particles break. Although the model does not simulate voids, or the kinematics accompanying the closure of voids, it is possible simply to add the component of energy dissipation due to fracture into an established constitutive relation which does model the deformation of a porous aggregate. For this purpose, a work equation (Roscoe *et al.*, 1963; Schofield and Wroth, 1968)

$$q\,\delta\varepsilon_q^p + p'\,\delta\varepsilon_v^p = Mp'\,\delta\varepsilon_q^p \tag{15}$$

is useful. The left hand side represents the work done per unit volume by deviatoric stress q and mean effective stress p' (with corresponding irrecoverable strain increments $\delta\varepsilon_q^p$ and $\delta\varepsilon_v^p$). The right hand side was identified as internal frictional dissipation. Schofield and Wroth's splitting of strains into plastic and elastic components can best be visualised in Fig. 3, where a one-dimensional compression of voids ratio δe is similarly decomposed into δe^p and δe^e.

If stress is monotonically increased from $\bar{\sigma}$ to $\bar{\sigma}+\mathrm{d}\bar{\sigma}$, $\log\bar{\sigma}$ increases by $\mathrm{d}\bar{\sigma}/\bar{\sigma}$ while a total change of voids ratio δe is observed. Schofield and Wroth invoked a potential elastic recovery of voids δe^e. They assumed local gradients λ and κ for the total and elastic strain legs in Fig. 3 and therefore calculated $\delta e = \lambda\,\mathrm{d}\bar{\sigma}/\bar{\sigma}$, $\delta e^e = \kappa\,\mathrm{d}\bar{\sigma}/\bar{\sigma}$, and deduced that the irrecoverable plastic component of voids ratio reduction is $\delta e^p = (\lambda-\kappa)\,\mathrm{d}\bar{\sigma}/\bar{\sigma}$. We will adopt the same approach, but will calculate the plastic component directly by defining

$$\delta e^p = \Lambda\,\mathrm{d}\bar{\sigma}/\bar{\sigma}, \tag{16}$$

and will shortly derive the conditions necessary for Λ to be a constant.

The assumption inherent in this approach is that recoverable strains are a function

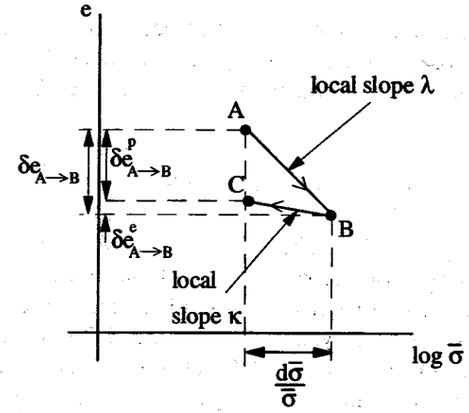

Fig. 3. Schofield and Wroth's decomposition of voids ratio reduction into elastic and plastic components.

of proportional change in stress, $\bar{\sigma}_B/\bar{\sigma}_A$ in Fig. 3, and not a function of the absolute value of stress.

We now add a term on the right hand side for the creation of surface energy due to fracture, and get

$$q\,\delta\varepsilon_q^p + p'\,\delta\varepsilon_v^p = Mp'\,\delta\varepsilon_q^p + \frac{\Gamma\,\mathrm{d}S}{V_s(1+e)}, \tag{17}$$

where $\mathrm{d}S$ is the change in surface area of a volume V_s of solids distributed in a gross volume of $V_s(1+e)$ where e is the voids ratio, and Γ is the "surface free-energy". For the special case of uniaxial deformation with effective axial stress $\bar{\sigma}$ and corresponding axial strain $\bar{\varepsilon}$ we obtain:

$$\bar{\sigma}\,\mathrm{d}\bar{\varepsilon}^p = \frac{2}{9}M(1+2K_0)\bar{\sigma}\,\mathrm{d}\bar{\varepsilon}^p + \frac{\Gamma\,\mathrm{d}S}{V_s(1+e)}, \tag{18}$$

where K_0 is the lateral/axial effective stress ratio. For the equilibrium of self-similar arrangements of rough rigid particles, it must be anticipated that K_0 would be solely a function of the internal angle of friction, ϕ. In soil mechanics it is accepted that $K_0 \approx 1-\sin\phi$ (Wroth, 1972). Substituting

$$\mathrm{d}\bar{\varepsilon}^p = -\frac{\mathrm{d}e^p}{(1+e)}, \tag{19}$$

we obtain

$$\mathrm{d}e^p = -\frac{\Gamma\,\mathrm{d}S}{(1-\mu)\bar{\sigma}V_s}, \tag{20}$$

where μ is a function of ϕ alone. Equation (20) may be expected to produce a reasonable approximation for confined one-dimensional compression. Miura and O-Hara (1979) showed in triaxial compression tests that for decomposed granite soil, the increase in surface area of the soil particles was proportional to the plastic work

done over most of the range of stresses considered. This is consistent with equation (20) and so the proposed relation can be used with confidence to establish the reduction in voids ratio e with increasing applied macroscopic compressive stress $\bar{\sigma}$.

3. NUMERICAL ANALYSIS

The initial array of 50 triangles is shown in Fig. 1. The initial co-ordination number of the triangles at the edges was set to three, so as to have the same chance of splitting as the particles in the bulk. For normalisation of the plots, the tensile strength σ_0 of the initial triangles was set at unity. Suppose a value of 5 is chosen for m. In order to explore how the voids ratio changes with $\bar{\sigma}$ at low values of $\bar{\sigma}$, it is useful first to calculate the stress such that only one triangle is likely to break. The initial survival probability for each triangle in the array should then be 0.98, and (13) gives the initial applied stress as:

$$\bar{\sigma} = \left\{\ln\left(\frac{1}{0.98}\right)\right\}^{1/m} = 0.458228 \quad \text{for } m = 5. \tag{21}$$

This has been selected as the starting point for the following analyses. It is essential to increment $\bar{\sigma}$ in very small amounts, but it is not necessary to use the same size of increment $d\bar{\sigma}$, for small and large $\bar{\sigma}$. Consequently, the increment was performed as:

$$\delta(\ln \bar{\sigma}) = 0.01. \tag{22}$$

In other words, the increment operation is:

$$\bar{\sigma} = \bar{\sigma}^{*}1.01. \tag{23}$$

For each increment of $\bar{\sigma}$, the program calculates the probability of fracture for each triangle. The program was written such as to generate a random number between 0 and 1, for each triangle under a current applied stress $\bar{\sigma}$. For example, if there were 100 triangles, all with a fracture probability of about 0.2, then if a random number between 0 and 1 is generated for each of the 100 particles, it would be expected that 20 of the outcomes would have a value of 0.2 or less. So if the condition for breakage is:

if random number $\leqslant$ probability of fracture, select particle for fracture

then the desired effect is achieved. This is the method adopted for selection for fracture. For each value of $\bar{\sigma}$, the particles were selected using the above method, and subsequently allowed to fracture. It was desired that this process be repeated until no more particles split. However, this was found to be too time-consuming, so the process was allowed to continue until the number breaking was less than 2% of the total number of particles. This was considered to give adequate accuracy.

The outcome of this procedure is almost exactly equivalent to invoking independent stochastic variations in both the forces acting on each particle, and in the strength of each particle. It is a feature of discrete element computations of elastic particles (Cundall and Strack, 1979) that contact forces vary strongly from particle to particle.

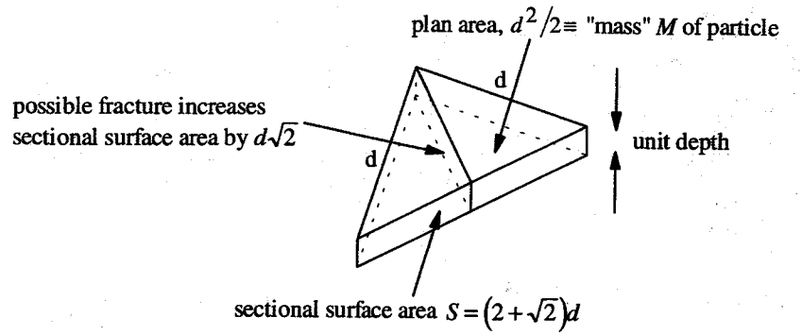

Fig. 4. The increase in sectional surface area when a triangle of shorter side d splits is $d\sqrt{2}$.

Strong columns of forces which are capable of transmitting the major compressive stress in the aggregate, form at intervals of a few particle diameters. Zones between columns are very lightly stressed. However, the organisation of columns must change whenever any particle fractures, so the snapshot of order at any instant should be irrelevant, and the process can be modelled as spatially random when integrated over hundreds of fractures.

In calculating the reduction in voids ratio for each increment of stress, it was noted that the new sectional surface area produced when a triangle splits, is proportional to the size of the triangle itself (Fig. 4).

If the orders of particle size are listed as $r = 0$ for the largest particle (size d_0) and $r = s$ for the smallest (size d_s), then (20) becomes

$$de \propto -\frac{\Gamma}{(1-\mu)\bar{\sigma}V_s}\sum_{r=0}^{r=s} B_r d_r, \tag{24}$$

where B_r is the number of particles of size d_r which are splitting.

It was decided to plot the particle size distribution after every 35 increments of stress, i.e. every time $\bar{\sigma}$ increased by a factor of about $\sqrt{2}(1.01^{35} \cong \sqrt{2})$. The change in voids ratio and uniformity coefficient, $U(U = d_{60}/d_{10}$, where d_{60} is the particle size which 60% by mass of the particles are finer than) were output after every increment of $\bar{\sigma}$.

4. ANALYSIS OF SIMULATIONS

It seemed reasonable to assume a value for m of 5 for soil particles and to vary parameter a controlling the influence of the co-ordination number on the probability of fracture. The results given in Fig. 5 are for $a = 5$. Results for $a = 4$ are shown in Fig. 6 for comparison. Wherever logarithmic axes appear in these figures, they are to the base 2, to match the concepts of binary splitting which underlie the theory. Figure 7 shows the resulting array of broken triangles for $a = 4$.

Figure 5(a) shows that the curves of percentage by number of particles larger than d, versus d on a logarithmic scale look like exponentials, as demonstrated by Fig. 5(b)

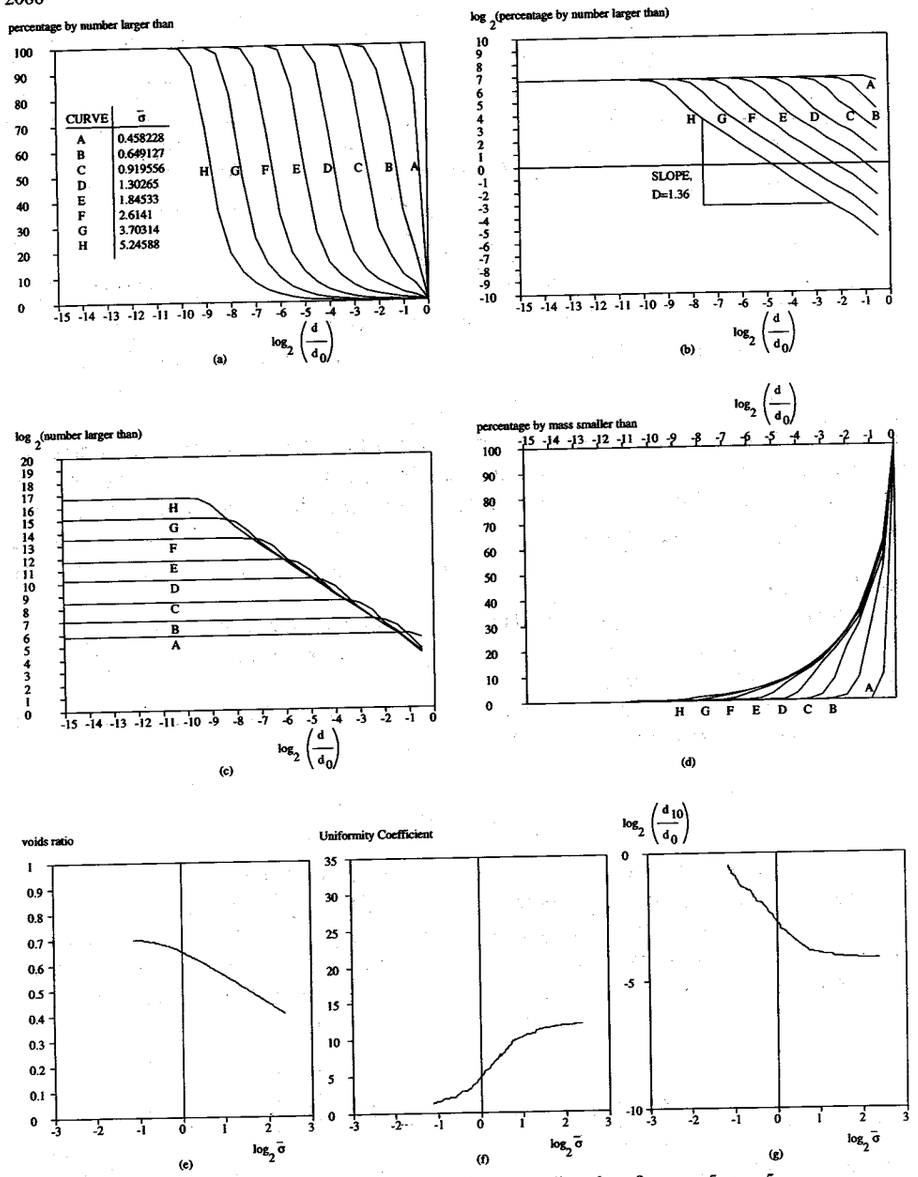

Fig. 5. Particle size distributions and compression data for $m = 5$, $a = 5$.

when the percentage by number of particles is also plotted on a logarithmic scale. This implies a fractal geometry. For a fractal distribution, the number of particles of size L greater than size d, $N(L > d)$ is given by:

$$N(L > d) = Ad^{-D}. \tag{25}$$

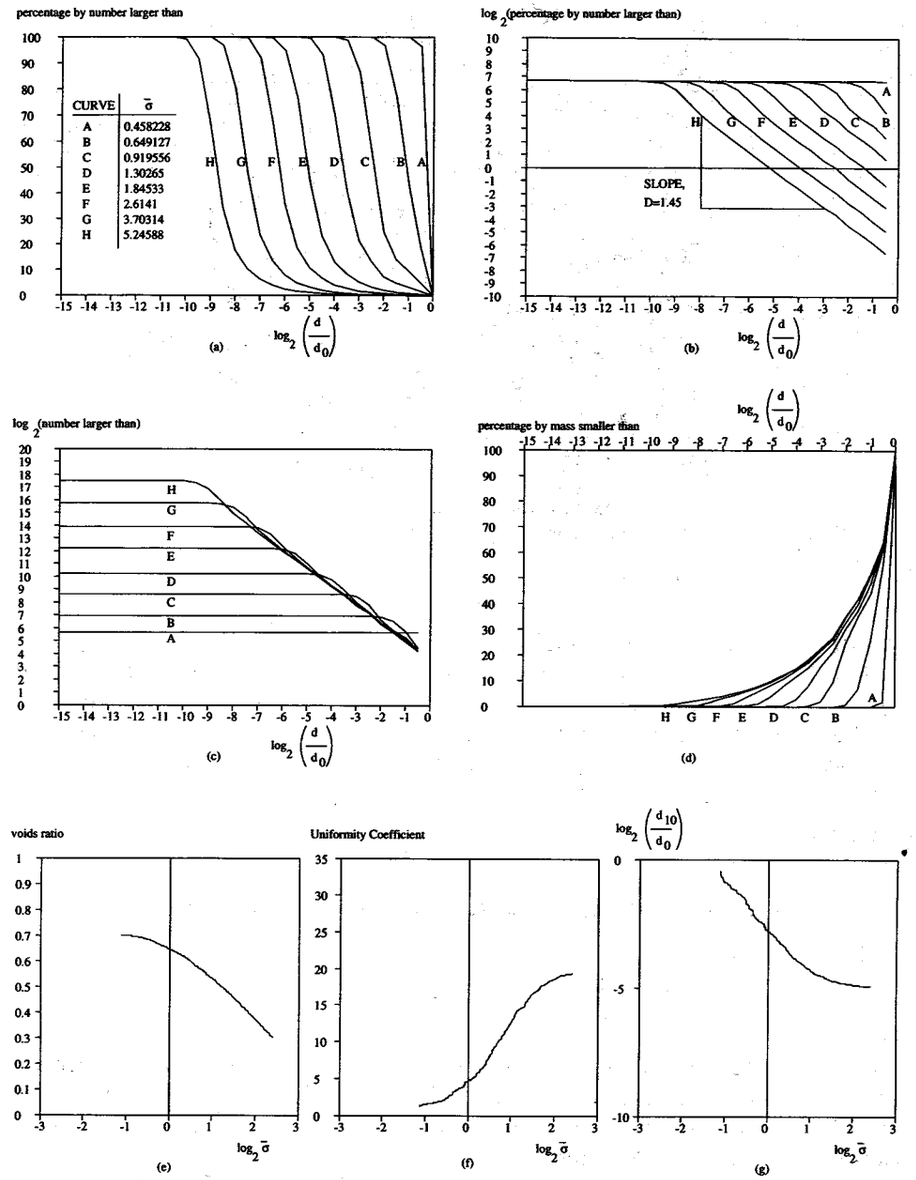

Fig. 6. Particle size distributions and compression data for $m = 5$, $a = 4$.

D is the fractal dimension, and has usually a value between 2 and 3 for granular materials (Turcotte, 1986). The constant of proportionality, A, is avoided in the literature, and it is necessary to ask whether it varies with loading. Figure 5(c) relates the logarithm of the absolute number of particles larger than d to the logarithm of d.

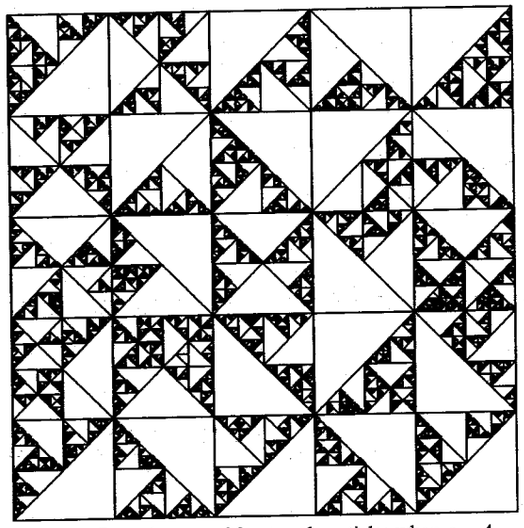

Fig. 7. Fractal array of fractured particles when $a = 4$.

Equation (25) corresponds to the sloping cut-off to each of the curves in Fig. 5(c), such that the slope and intercept at every stress level is identical, and (25) forms an envelope with a unique value of both A and D for every test. Only the smaller particles are fracturing each time the applied stress $\bar{\sigma}$ is incremented, because the high co-ordination numbers of the larger particles give them low probabilities of fracture. If the smallest particle size under a particular value of stress is d_s, then

$$N(L > d_s) = Ad_s^{-D}. \tag{26}$$

Hence the fraction of particles of size greater than d, $\Phi_{L>d}$ is given by:

$$\Phi_{L>d} = \frac{N(L > d)}{N(L > d_s)} = \left(\frac{d}{d_s}\right)^{-D}. \tag{27}$$

The nature of (27) ensures that the curves in Fig. 5(a) are at equal horizontal spacings. If the logarithm of (27) is calculated, and plotted as in Fig. 5(b), then the value of the fractal dimension, D, emerges again as the slope. For $m = 5$ and $a = 5$, D was calculated to be 1.36, whilst for $m = 5$ and $a = 4$, D was found to be 1.45. This is reasonable because the fractal dimension can be calculated from the fractal probability of fracture p, and the number of fragments n produced when a particle breaks. Palmer and Sanderson (1991) showed that if the particle sizes are numbered from d_0 for the largest particle to d_s as the smallest particle, then:

$$\frac{N(L > d_i)}{N(L > d_{i+1})} = \left(\frac{d_i}{d_{i+1}}\right)^{-D} = (n^{1/w})^{-D} = \frac{1}{np}, \tag{28}$$

where $w = 2$ in two dimensions and $w = 3$ in three dimensions—see (5). Hence D is calculated as

$$D = w\left(1 + \frac{\ln p}{\ln n}\right). \tag{29}$$

In two dimensions, D is expected to lie between 0 and 2, and for the fracture of three-dimensional grains D is expected to lie between 0 and 3 (as indicated by Palmer and Sanderson).

Palmer and Sanderson's model suggests that the number of orders of particles produced increases with applied stress. So it is with the model presented here. As the applied stress $\bar{\sigma}$ increases, the probability of fracture for the smallest particles must be the same each time they fracture. Consequently, Palmer's fractal probability of fracture can be related to Weibull's survival probability in (13) for the 2D crushing of triangles:

$$1 - p = P_s = \exp\left\{-\left(\frac{d_s}{d_0}\right)^2 \frac{(\bar{\sigma}/\sigma_0)^m}{(C-2)^a}\right\}. \tag{30}$$

Equation (30) suggests the following relation between finest particle size and applied stress:

$$\frac{d_s^2 \bar{\sigma}^m}{d_0^2 \sigma_0^m} = \ln\left[\frac{1}{1-p}\right] = f, \tag{31}$$

where

$$p = n^{(D/2-1)}. \tag{32}$$

Equation (31) can be written as:

$$d_{s-j}^2 \bar{\sigma}^m = \text{constant}, \tag{33}$$

where $0 \leqslant j \leqslant s$ and j is a constant. This rule predicts that size distribution curves in Fig. 5(a) should be of constant shape, translating to the left by equal amounts as stress increases by equal increments. In this sense, fractal self-similarity has emerged from the initially uniform triangular array by the stage of curve C in Fig. 5(a), when the normalised compressive stress is about unity (i.e. equal to the tensile strength of the particles). A similar early transition into fractal numbers is found in Fig. 6(a). Furthermore, a repetition of these numerical simulations using different Weibull moduli m, confirmed that the spacing of distribution curves increased with increasing m exactly as predicted by (31).

The cumulative mass fraction curve in Fig. 5(d) appears to show that as the grain size distribution curves evolve, they are tending towards a stable exponential curve. This is to be expected. If there are a differential number of particles δN of size between d and $d+\delta d$, then from (25),

$$\delta N = ADd^{-D-1}\,\delta d. \tag{34}$$

Integrating equation (34) between particle sizes d and ∞, (25) is obtained. The corresponding differential mass δM is:

$$\delta M = 0.5\,\mathrm{d}N \cdot d^2 = 0.5ADd^{1-D}\,\delta d. \tag{35}$$

The term "mass", which here refers to the plan areas of particles in the 2D simulation, as shown in Fig. 4, has been used so as to link with literature on particle size analysis. Integrating (35), the mass of particles finer than a particle size d, $M(L < d)$ is obtained as:

$$M(L < d) = \frac{ADd^{2-D}}{2(2-D)}. \tag{36}$$

Since A and D are constant, (36) gives the final mass distribution of particle sizes, which will be approached as the smallest particles continue breaking on each increment of applied stress. As a result, the uniformity coefficient approaches a constant value as shown in Fig. 5(f).

The plot of voids ratio against logarithm of applied stress is shown in Fig. 5(e). Initial voids ratio indicates the state of packing of grains which is not recognised by the simulation; an arbitrary but typical value of 0.7 was selected. The curve has the expected shape, with less crushing evident at lower stresses, and the amount of breakage increasing as $\bar{\sigma}$ increases and fractals begin to form. It is possible to express the form of the curve representing fractal crushing in a closed form. For the differential number of particles between size d and $d+\delta d$, given by (34), the corresponding sectional surface area δS is:

$$\delta S = \beta ADd^{-D}\,\delta d, \tag{37}$$

where $\beta = 2+\sqrt{2}$, as shown in Fig. 4. The total sectional area for particles size d and greater, $S(L > d)$ is:

$$S(L > d) = \frac{\beta ADd^{1-D}}{D-1}. \tag{38}$$

The total sectional area, then, for all the particles in the sample is:

$$S(L > d_s) = \frac{\beta ADd_s^{1-D}}{D-1}. \tag{39}$$

Combining (31) and (39),

$$S(L > d_s) = \frac{\beta f^{(1-D)/2} AD}{D-1} d_0^{1-D} \left(\frac{\bar{\sigma}}{\sigma_0}\right)^{m(D-1)/2}. \tag{40}$$

Putting (40) into (20), the plastic reduction in voids ratio with applied stress increment, $\mathrm{d}\bar{\sigma}$ is:

$$\mathrm{d}e^p = -\beta f^{(1-D)/2} \frac{\Gamma}{(1-\mu)\bar{\sigma}V_s} AD\frac{m}{2} d_0^{1-D} \sigma_0^{m(1-D)/2} (\bar{\sigma})^{m(D-1)/2-1}\,\mathrm{d}\bar{\sigma}, \tag{41}$$

Substituting for V_s as the mass of particles of size less than or equal to d_0 [equation (36)] in (41),

$$\mathrm{d}e^p = -\beta f^{(1-D)/2} \frac{\Gamma}{(1-\mu)\bar{\sigma}d_0} (2-D) m \sigma_0^{m(1-D)/2} (\bar{\sigma})^{m(D-1)/2-1}\,\mathrm{d}\bar{\sigma}, \tag{42}$$

which can be written

$$\mathrm{d}e^p = -\Lambda(\bar{\sigma})^{m(D-1)/2-1} \frac{\mathrm{d}\bar{\sigma}}{\bar{\sigma}} \tag{43}$$

where

$$\Lambda = \beta f^{(1-D)/2} \frac{\Gamma}{(1-\mu)d_0} (2-D) m \frac{1}{\sigma_0^{m(D-1)/2}}. \tag{44}$$

In the particular case

$$D = \frac{2}{m} + 1 \tag{45}$$

(43) reduces to (16) and can be integrated to give an equation similar in form to (1).

It was found that the value of fractal dimension, D, was strongly influenced by the value of a chosen as the power of the co-ordination function, but the value of Weibull modulus m had no effect. As a result, for a given value of a (i.e. D), it would be possible to use (45) to deduce the corresponding value of m which gives a linear e–$\log\bar{\sigma}$ plot. Changing the value of a at this selected value of m introduces curvature to the plot. This provides a micro mechanical commentary for the empirical observation that some granular materials do not exactly follow linear compression lines on e–$\log\bar{\sigma}$ plots.

In three dimensions, the use of $w = 3$ in (5) and the consistent definition of volume as a cubic function of linear dimension, causes (45) to become

$$D = \frac{3}{m} + 2. \tag{46}$$

For most soils, m will be between 5 and 10; D is often around 2.5 (Turcotte, 1986; Palmer and Sanderson, 1991), and these values fit (46) rather well. It must therefore be reasonable to propose that the difference in linearity between normal compression curves for various soils of equal fractal dimension may be due to the difference in the variability of the tensile strengths of the particles themselves. Equation (44) shows that the plastic compressibility index Λ increases with increasing Weibull modulus m (i.e. decreasing variability in particle tensile strength). Furthermore, accepting that $\sigma_0 \propto \sqrt{\Gamma}$ from linear-elastic fracture mechanics principles (Griffith, 1920), (44) gives the dependence of Λ on toughness, Γ as:

$$\Lambda \propto \Gamma^{1-m(D-1)/4}, \tag{47}$$

which in the case of ideal Λ-lines which satisfy (45) exactly, leads to the proposition

$$\Lambda \propto \sqrt{\Gamma}. \tag{48}$$

It is possible to substitute typical values of parameters into (44) in order to check that the plastic compression index Λ has the right order of magnitude. For example, Lee (1992) showed that the expected strength of a quartz sand particle of diameter 0.5 mm would be $\sigma_0 = 50$ MPa; the surface free-energy Γ of silicates is of the order of 50 J/m^2 [Ashby and Jones, 1986], the coefficient μ from (18) can be taken to be 0.5 using $M = 1$ and $K_0 = 0.6$, the Weibull modulus m can be taken to be 8 and the fractal dimension $D = 1.25$ for the 2D simulation to achieve ideal, linear Λ-lines. These substitutions give $\Lambda \sim 0.1$ which is of the correct order, comparing with available data of both sands and clays.

For the two sets of data shown in Figs 5 and 6, it is evident that decreasing the value of a (i.e. for a given value of m, decreasing α) causes more grain crushing. More large particles are allowed to break, and the final mass distribution is approached less quickly because the final uniformity coefficient is larger and the fractal dimension is higher. The resulting compression is greater, as illustrated on the e–log $\bar{\sigma}$ plots. This may be taken to illustrate the difference between a material composed of rounded particles and one composed of angular particles. Angular particles are inherently more susceptible to breakage and less influenced by the co-ordination number, and the resulting compression is larger than for a sample of rounded particles (Lee and Farhoomand, 1967). This reinforces the idea suggested in Section 2 that the value of α could be selected with respect to the shape of the particles.

5. DISCUSSION

It should be noted that the results discussed so far have been for values of a greater than 2. It was found that as a decreased, D increased. At a value of $a = 2$, D was estimated to be close to 2.0. This corresponds to a situation in which the particle size and co-ordination number are equally important in determining the fragment size distribution. Consider a situation as shown in Fig. 8(a) where a particle P of size d is surrounded by three particles of equal size and co-ordination number [and hence equal probability of fracture—see (13)]. Now suppose that P splits such as to increase the co-ordination number of each of its neighbours by one [Fig. 8(b)]. Equation (13)

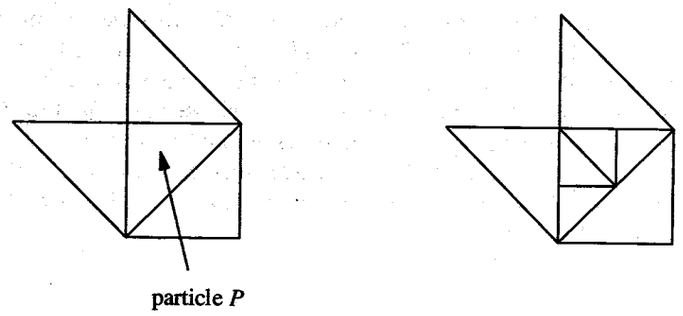

Fig. 8. Particle P splits such as to increase the co-ordination number of each of its neighbours by one.

suggests that if each of the particles is now to have the same probability of splitting, then

$$\left(\frac{d}{d_0}\right)^2 \frac{(\sigma/\sigma_0)^m}{(4-2)^a} = \left(\frac{d/2}{d_0}\right)^2 \frac{(\sigma/\sigma_0)^m}{(3-2)^a}, \tag{49}$$

i.e. $a = 2$. If $a \ll 2$, then clearly the larger particles have a greater probability of splitting, and this will tend to scavenge the larger particles out of the aggregate. For $a \gg 2$, the smaller particles are more likely to fracture, so that some large particles are retained under the protection of their neighbours. It must be emphasised that all signs of fractal behaviour do not just suddenly disappear at $a = 2$, nor is (49) meant to be a formal proof of the existence of a watershed. It has simply been demonstrated that as a decreases beyond a value of about 2, it should be expected that the deviation from fractal behaviour becomes more and more pronounced. Consequently, on a log–log plot of the percentage by number of particles larger than a given size [as in Fig. 5(b)], no unique value of D can be found. This is reassuring because a value of D greater than 2 has no meaning for a fractal distribution in two dimensions anyway [equation (29)]. However, the idea that particle size is more dominant than co-ordination number in determining the fracture probability of a particle, is considered unrealistic. Billam (1971) found that for the grain degradation of granular materials, the larger grains often suffered little crushing, even at very high pressures. Palmer and Sanderson (1991) also noted that in the case of ice-structure interaction, ice appears to be pulverised in the crushed zone. They stated that there is no evidence to suggest that large particles are absent, but that there are simply a large number of small fragments which determine the superficial appearance of the crushed zone.

It should now be clear that the choice of co-ordination number function is irrelevant, provided the co-ordination number dominates over particles size in the determination of the survival probability of a particle. In this case (31)–(48) apply. For the chosen function of $(C-2)^a$, then, it is necessary to compare the curves obtained for $a > 2$ with corresponding grading curves and compression plots found by experiment.

Figure 9 (Fukumoto, 1992) shows the evolving grading curves for one-dimen-

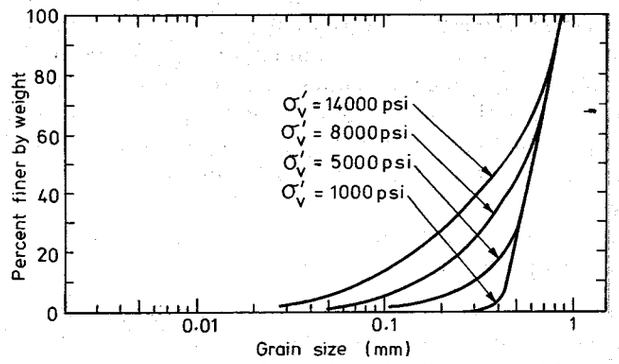

Fig. 9. Evolving particle size distribution curves for one-dimensionally compressed Ottawa sand (Fukumoto 1992).

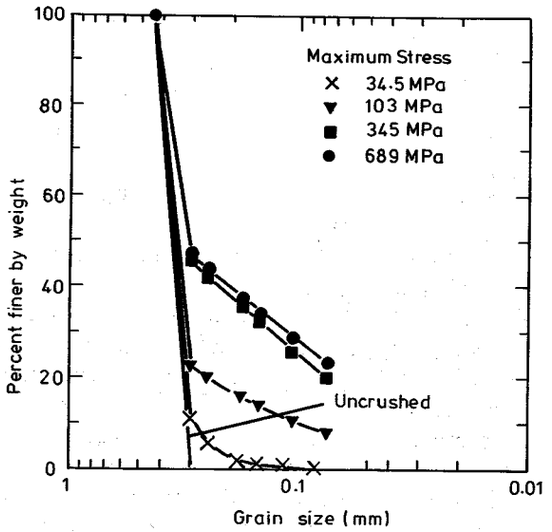

Fig. 10. Evolving particle size distribution curves for one-dimensionally compressed glass beads (Hagerty *et al.* 1993).

sionally compressed Ottawa sand. The comparison with Fig. 5(d) is good. Similar evolving curves are given by Hagerty *et al.* (1993) for glass beads (Fig. 10) and for Black Beauty Slag. Hagerty *et al.* also showed that angular glass beads are more readily susceptible to breakage than round glass beads, with more larger particles breaking. By choosing a lower value of a (e.g. 2.2), it is possible to model this effect. Lee and Farhoomand (1967) have presented photographs to show that the number of fines produced is greater for an angular sand than for a rounded sand, with more large particles breaking and a higher compressibility. In comparing Figs 5(d) and 6(d), and Figs 5(e) and 6(e), it is evident that these plots illustrate this difference in behaviour between angular and rounded granular materials. Golightly (1990) shows in Fig. 11 a typical e–$\log \bar{\sigma}$ plot for carbonate sands. Figure 12 shows a similar plot by Biarez and Hicher (1994) for petroleum coke. The plot also shows values of uniformity coefficient increasing to a constant value at lower void ratios (the change in curvature of the plot with a reduction in uniformity coefficient at very low voids ratios is probably due to the communition limit for petroleum coke). The data are seen to be in good qualitative agreement with Figs 5(e), (f) and 6(e), (f). Furthermore, it may be perceived that recoverable strains are small in relation to plastic strains, thus justifying their omission from the e–$\log \bar{\sigma}$ plots derived by the simulation—at least in this case.

It is appropriate to recall the features of soil behaviour, which have been omitted from this simple treatment, however:

(i) The initial voids ratio has not been linked to the initial co-ordination number of particles, nor has the anisoptropic distribution of contact normals explicitly been considered.

(ii) The solution has relied upon the empirical finding $\bar{\sigma}_3/\bar{\sigma}_1 = K_0 = 1 - \sin\phi$ for

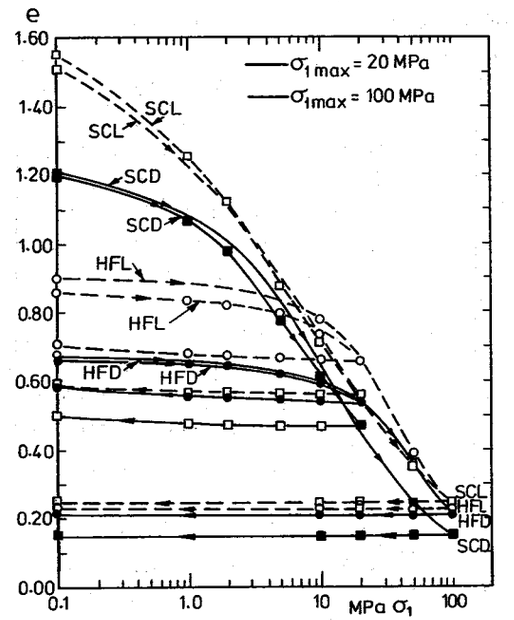

SCD= Dense carbonate sand SCL=Loose carbonate sand
HFD=Dense silica sand HFL=Loose silica sand

Fig. 11. Typical one-dimensional compression curves for carbonate sands (Golightly, 1990).

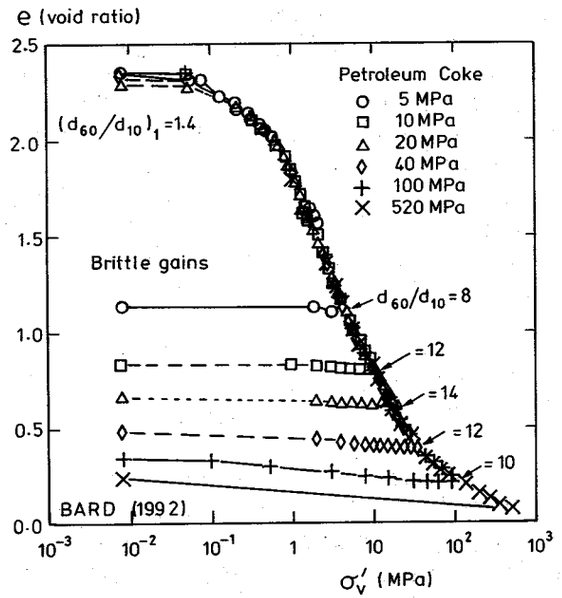

Fig. 12. Typical e–$\log \bar{\sigma}$ plot for petroleum coke, showing uniformity coefficient increasing to a constant value before the comminution limit is reached (Biarez and Hicher, 1994).

one-dimensional compression. Further consideration must in future be given to the definition of a yield surface which would generalise the results presented here.

(iii) No attempt has been made to describe the unstable release of elastic strain energy, and the subsequent unstable collapse of grains, which may well be expected to follow the fracture of a single particle. Instead, the hundreds and thousands of fractures which are typically produced during the doubling of stress are integrated and their effects smoothed. Following a local collapse the locally reduced strain energy must begin to build up again, and it is assumed that the average elastic strain energy (over a volume much larger than a single particle) will be a smooth function of the applied stress.

(iv) Recoverable reduction of voids ratio can be added to the plastic reduction calculated as a result of fracture; Hertzian contact mechanics will clearly assist. However, it is the plastic voids compression index Λ which has been calculated here, and the distinction between Λ and the total voids compression index λ has currently been left unexplored.

Not withstanding these limitations, the probability of fracture of a soil grain has proved a remarkably fertile starting point for a re-evaluation of plastic hardening in soil mechanics. Critical state soil mechanics, developed in Cambridge from 1958 to 1969, associated stress and voids ratio. The successive crushing model presented here additionally associates a distribution of particle sizes to each stress, and postulates that plastic hardening is due to the increase of specific surface which must accompany the irrecoverable compression due to particle breakage.

No other treatment of the mechanics of granular media has been able to explain the existence of linear-log compression lines for soils. It is tempting to apply a reverse argument and to infer that the characteristically linear e–$\log \bar{\sigma}$ for clays should be explained in terms of fractal crushing. Clays are widely recognised to form "peds"—groups of individual particles of size ≈ 1 μm which form a large bonded unit of size ≈ 10 μm (Fig. 13). Furthermore, studies of pore size distributions (Akagi, 1994) have shown that compression of the fabric leads to the elimination of the larger macro-pores while the distribution of micro-pores remains unchanged. All this is consistent with the view that a clay ped be recognised as the basic granular unit, that peds should be treated as crushable grains, and that the compression of clays be regarded as the fractal crushing of peds. It seems to be necessary to view the "plasticity" of soils described by Schofield and Wroth (1968) as a corollary of the fracture of "grains".

6. CONCLUSIONS

A conceptual model has been developed for the evolution of a granular medium under stress as a function of the behaviour of individual grains. A statistical treatment has been provided in which the probability of fracture is a function of applied stress, particle size and co-ordination number. A highly simplified numerical simulation ignores the effects of voids, and the details of equilibrium and kinematics local to a particle: a conventional continuum work equation is used instead to describe inte-

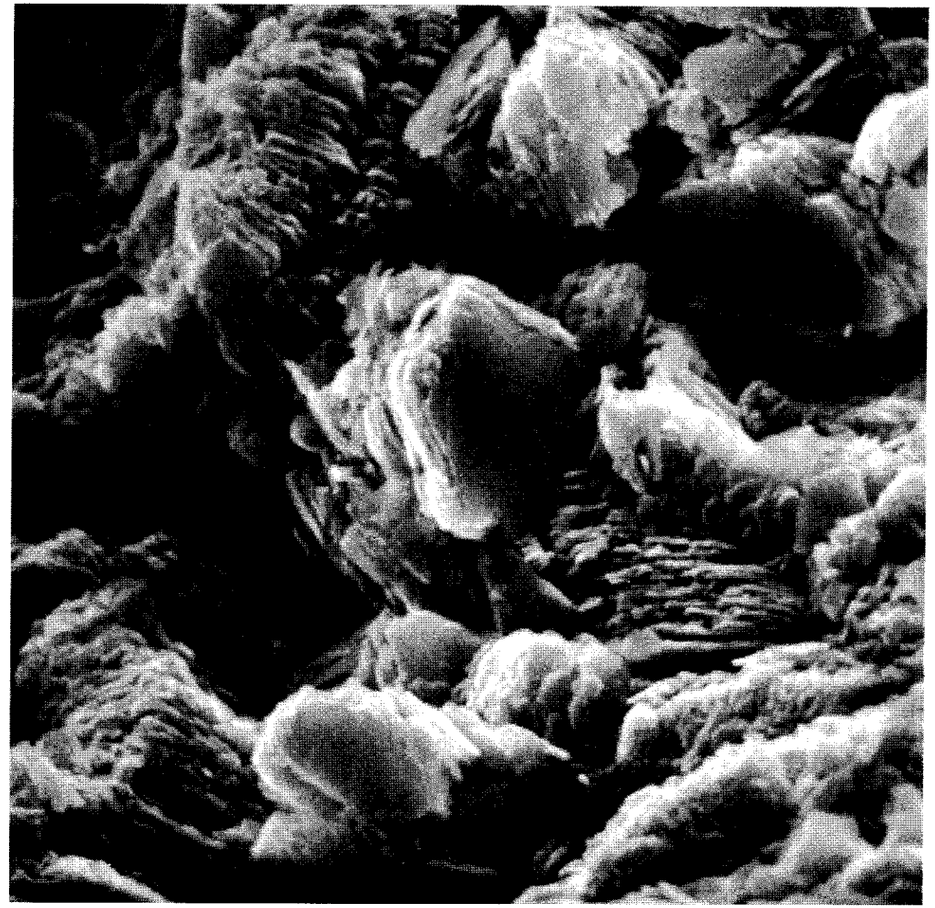

Fig. 13. Scanning electron micrograph (picture width 50 μm) of undisturbed Kaolin, showing a random distribution of orientated peds (Tovey, 1971).

grated effects. Nevertheless it has proved capable of modelling significant aspects of one-dimensional compression of granular materials by particle crushing.

When the effect of co-ordination number dominates over particle size in determining the probability of fracture for a particle, the resulting particle size distributions are fractal in nature with realistic fractal dimensions. By choosing appropriate particle parameters, it is possible to obtain particle size distributions and normal compression curves which resemble those found experimentally.

The successive fracture of brittle soil particles to form a fractal geometry gives a micro mechanical basis for the observation that the compression of a granular aggregate is proportional to the logarithm of applied stress. A relationship has been proposed between the compressibility of a granular material and its more fundamental particle properties. Theory shows that the compressibility of the aggregate will depend on fractal dimension D, the particle material toughness Γ, the variability in particle tensile strength m, and the angle of friction of the soil, ϕ.

The model could readily be extended to investigate the crushing of a soil composed of more than one species, and a comminution limit could be added, making it possible to model the one dimensional compression of granular materials over the full range of voids ratios.

ACKNOWLEDGEMENTS

Glenn McDowell thanks the EPSRC for the financial support of a studentship. The authors are grateful to Hewlett Packard for their donation of a computer, and for their stimulation of the COLOS (Conceptual Learning of Science) initiative.

REFERENCES

Akagi, H. (1994) A physico-chemical approach to the consolidation mechanism of soft clays. *Jap. Soc. Soil Mech. Foundation Engng* **34**(4), 43–50.

Ashby, M. F. and Jones, D. R. H. (1986) *Engineering Materials* 2. Pergamon Press, Oxford.

Biarez, J. and Hicher, P. (1994) *Elementary Mechanics of Soil Behaviour*. A. A. Balema, Rotterdam.

Billam, J. (1971) Some aspects of the behaviour of granular materials at high pressures. *Stress–strain behaviour of soils. Proc. Roscoe Memorial Symposium* (ed. R. H. G. Parry), pp. 69–80.

Cundall, P. A. and Strack, O. D. L. (1979) A discrete numerical model for granular assemblies. *Geotechnique* **29,** 47–65.

Epstein, B. (1949) The mathematical description of certain breakage mechanisms leading to the logarithmico-normal distribution. *J. Franklin Inst.* **244,** 471–477.

Fukumoto, T. (1992) Particle breakage characteristics in granular soils. *Soils and Foundations* **32**(1), 26–40.

Gilvarry, J. J. (1961) Fracture of brittle solids, I. Distribution function for fragment size in single fracture (theoretical). *J. Appl. Phys.* **32,** 391–399.

Gilvarry, J. J. (1964) Distribution of fragment size in repetitive fracture of brittle solids. *Solid State Commun.* **2,** 9–11.

Golightly, C. R. (1990) Engineering properties of carbonate sands. Ph.D. dissertation, Bradford University.

Griffith, A. A. (1920) The phenomena of rupture and flow in solids. *Philos. Trans. R. Soc. Lond. A* **221,** 163–198.

Hagerty, M. M., Hite, D. R., Ullrich, C. R. and Hagerty, D. J. (1993) One dimensional compression of granular media. *J. Geotechnical Engng, ASCE* **119,** 1–18.
Hardin, B. O. (1985) Crushing of soil particles. *J. Geotechnical Engng, ASCE* **111,** 1177–1192.
Jaeger, J. C. (1967) Failure of rocks under tensile conditions. *Int. J. Rock. Min. Sci.* **4,** 219–227.
Lee, D. M. (1992) The angles of friction of granular fills. Ph.D. dissertation, Cambridge University.
Lee, K. L. and Farhoomand, I. (1967) Compressibility and crushing of granular soil. *Canadian Geotechnical Journal* **4,** 68–86.
McGlade, J. M. (1993) Alternative Ecologies. *New Scientist Supplement* **137** (1980), 14–16.
Miura, N. and O-Hara, S. (1979) Particle-crushing of a decomposed granite soil under shear stresses. *Soils and Foundations* **19**(3), 1–14.
Novello, E. A. and Johnston, I. W. (1989) Normally consolidated behaviour of geotechnical materials. *Proc. 12th Int. Conf. Soil Mech., Rio de Janeiro* **3,** 2095–2100.
Palmer, A. C. and Sanderson, T. J. O. (1991) Fractal crushing of ice and brittle solids. *Proc. R. Soc. Lond. A* **433,** 469–477.
Roscoe, K. H., Schofield, A. N. and Thurairajah, A. (1963) Yield of clays in states wetter than critical. *Geotechnique* **13,** 211–240.
Sammis, C., King, G. and Biegel, R. (1987) The kinematics of gouge deformation. *Pure Appl. Geophys.* **125,** 777–812.
Schofield, A. N. and Wroth, C. P. (1968) *Critical State Soil Mechanics.* McGraw-Hill, London.
Tovey, N. K. (1971) A selection of scanning electron micrographs of clays. Cambridge University Engineering Department Technical Report CUED/C-SOILS/TR5.
Turcotte, D. L. (1986) Fractals and Fragmentation. *J. Geophysical Res.* **91,** 1921–1926.
Weibull, W. (1951) A statistical distribution function of wide applicability. *J. Appl. Mech.* **18,** 293–297.
Wroth, C. P. (1972) General theories of earth pressure and deformations. *Proc. 5th Eur. Conf S.M.F.E.* **2,** 23–52.